Developmental Biology 363 (2012) 388–398

Contents lists available at SciVerse ScienceDirect

Developmental Biology

journal homepage: www.elsevier.com/developmentalbiology

Multiple RNA-binding proteins function combinatorially to control the soma-restricted expression pattern of the E3 ligase subunit ZIF-1

Marieke Oldenbroek, Scott M. Robertson, Tugba Guven-Ozkan [1], Steven Gore, Yuichi Nishi [2], Rueyling Lin *

Department of Molecular Biology, University of Texas Southwestern Medical Center, Dallas, TX 75390, USA

ARTICLE INFO

Article history:
Received for publication 8 August 2011
Revised 2 January 2012
Accepted 3 January 2012
Available online 12 January 2012

Keywords:
zif-1
Translational repression
C. elegans
Embryos
Germline
POS-1
MEX-5/6
MEX-3
SPN-4
PIE-1

ABSTRACT

In *C. elegans* embryos, transcriptional repression in germline blastomeres requires PIE-1 protein. Germline blastomere-specific localization of PIE-1 depends, in part, upon regulated degradation of PIE-1 in somatic cells. We and others have shown that the temporal and spatial regulation of PIE-1 degradation is controlled by translation of the substrate-binding subunit, ZIF-1, of an E3 ligase. We now show that ZIF-1 expression in embryos is regulated by five maternally-supplied RNA-binding proteins. POS-1, MEX-3, and SPN-4 function as repressors of ZIF-1 expression, whereas MEX-5 and MEX-6 antagonize this repression. All five proteins bind directly to the *zif-1* 3′ UTR in vitro. We show that, in vivo, POS-1 and MEX-5/6 have antagonistic roles in ZIF-1 expression. In vitro, they bind to a common region of the *zif-1* 3′ UTR, with MEX-5 binding impeding that by POS-1. The region of the *zif-1* 3′ UTR bound by MEX-5/6 also partially overlaps with that bound by MEX-3, consistent with their antagonistic functions on ZIF-1 expression in vivo. Whereas both MEX-3 and SPN-4 repress ZIF-1 expression, neither protein alone appears to be sufficient, suggesting that they function together in ZIF-1 repression. We propose that MEX-3 and SPN-4 repress ZIF-1 expression exclusively in 1- and 2-cell embryos, the only period during embryogenesis when these two proteins co-localize. As the embryo divides, ZIF-1 continues to be repressed in germline blastomeres by POS-1, a germline blastomere-specific protein. MEX-5/6 antagonize repression by POS-1 and MEX-3, enabling ZIF-1 expression in somatic blastomeres. We propose that ZIF-1 expression results from a net summation of complex positive and negative translational regulation by 3′ UTR-binding proteins, with expression in a specific blastomere dependent upon the precise combination of these proteins in that cell.

Introduction

Beginning with the zygote, P0, a series of four asymmetric divisions specifies P4, the single founder blastomere for the entire germline in *C. elegans* (Strome, 2005). Each of these divisions generates a smaller germline precursor (P1 through P4, termed the P lineage) and a larger somatic sister cell (Fig. 1A). P4 divides symmetrically to generate Z2 and Z3, which go on to generate the entire germline post-embryonically. All P lineage germline blastomeres are transcriptionally repressed, a defining characteristic of primordial germ cells (Nakamura and Seydoux, 2008; Seydoux and Fire, 1994). Their somatic sisters, however, undergo rapid transcriptional activation and lineage-specific differentiation, demanding rapid reversibility for any repressive mechanism operating in the P lineage (Seydoux and Fire, 1994).

Transcriptional repression in the *C. elegans* germline precursors requires at least two classes of maternally-supplied proteins. In P0 and P1, two closely-related and functionally redundant CCCH tandem zinc finger proteins, OMA-1 and OMA-2, globally repress transcription initiation by sequestering TAF-4, a critical component of the RNA pol II preinitiation complex, in the cytoplasm (Guven-Ozkan et al., 2008). In P2–P4, PIE-1, another CCCH tandem zinc finger protein, globally represses transcription by inhibiting both initiation and elongation phases of transcription (Batchelder et al., 1999; Ghosh and Seydoux, 2008; Seydoux and Dunn, 1997; Zhang et al., 2003). OMA-1, OMA-2, and PIE-1 proteins are all expressed from maternally-supplied mRNAs and are first detected in developing oocytes (Detwiler et al., 2001; Mello et al., 1996). OMA-1 and OMA-2 are degraded soon after the first mitotic division and are not detected in subsequent P lineage blastomeres (Detwiler et al., 2001; Lin, 2003). Degradation requires phosphorylation of the OMA proteins by at least two kinases, one of which, the DYRK2-type kinase MBK-2, is developmentally activated in newly-fertilized one-cell embryos (Cheng et al., 2009; Nishi and Lin, 2005; Shirayama et al., 2006; Stitzel et al., 2006). PIE-1 is segregated preferentially to the germline blastomere at each P lineage division (Mello et al., 1996). Global transcriptional repression by both OMA and PIE-1 is a robust but readily reversible way to transcriptionally silence the germline precursors, while maintaining

* Corresponding author. Fax: +1 214 648 1196.
E-mail address: Rueyling.Lin@UTSouthwestern.edu (R. Lin).
[1] Current address: Dept. of Neuroscience, The Scripps Research Institute, Jupiter, FL 33458, USA.
[2] Current address: Dept. of Molecular and Cellular Biology, Harvard University, Cambridge, MA 02138, USA.

0012-1606/$ – see front matter © 2012 Elsevier Inc. All rights reserved.
doi:10.1016/j.ydbio.2012.01.002

the chromatin primed for transcriptional activation in the somatic sisters (Schaner et al., 2003).

The germline blastomere specific localization of PIE-1 is the result of selective enrichment towards the presumptive germline blastomere prior to division, coupled with selective degradation of any PIE-1 remaining in the somatic blastomeres following division (Reese et al., 2000). Degradation of PIE-1 in somatic cells is initiated by a CUL-2 containing E3 ligase (DeRenzo et al., 2003). The substrate-binding subunit of this E3 ligase, ZIF-1, binds PIE-1 via the first of the two CCCH zinc fingers found in PIE-1 (DeRenzo et al., 2003). GFP fused to the first zinc finger of PIE-1 (GFP::PIE-1 ZF1) functions as a reporter for PIE-1 degradation and undergoes ZIF-1-dependent degradation specifically in somatic blastomeres (Reese et al., 2000). We showed recently that the spatial and temporal regulation of this E3 ligase activity is controlled at the level of *zif-1* translation (Guven-Ozkan et al., 2010). In *C. elegans*, correct spatio-temporal expression of almost all maternally-supplied transcripts is regulated post-transcriptionally via the 3′ UTR (Merritt et al., 2008). Using a translational reporter containing the *zif-1* 3′ UTR, we showed that *zif-1* is translated in somatic cells, where PIE-1 is degraded, but not in oocytes or germline blastomeres, where PIE-1 levels are normally maintained.

We recently showed that OMA-1 and 2 bind to the *zif-1* 3′ UTR and, in a SPN-2 dependent manner, repress translation of *zif-1* in oocytes (Guven-Ozkan et al., 2010;Li et al, 2009). This repression is relieved by phosphorylation of OMA-1 and -2 by MBK-2 (Guven-Ozkan et al., 2010). OMA proteins are phosphorylated by MBK-2 soon after completion of meiosis II, and therefore it is unlikely that they are responsible for the continuing repression of *zif-1* translation in 1-cell embryos. It is not known how *zif-1* translation remains repressed in 1- and 2-cell embryos, and is asymmetrically activated only in somatic blastomeres at the 4-cell stage. Many maternally-supplied key regulators of early embryonic patterning identified through forward genetic screens turned out to be proteins with RNA-binding motifs, highlighting the critical importance of translational control in early embryogenesis. Most of these RNA-binding proteins are asymmetrically localized to one or a few blastomeres. For example, POS-1, MEX-1, and SPN-4 are localized primarily to germline blastomeres (Guedes and Priess, 1997; Ogura et al., 2003; Tabara et al., 1999), whereas MEX-3, MEX-5, and MEX-6 are localized primarily to somatic blastomeres (Draper et al., 1996; Schubert et al., 2000). POS-1, MEX-1, MEX-5, and MEX-6, like PIE-1, all contain tandem CCCH zinc-finger RNA-binding motifs, and all are targets of the ZIF-1 containing E3 ligase (DeRenzo et al., 2003; Guedes and Priess, 1997; Mello et al., 1996; Reese et al., 2000; Schubert et al., 2000; Tabara et al., 1999). ZIF-1-dependent degradation in somatic blastomeres contributes to the restricted localization pattern of these proteins. MEX-5/6 are the only ZIF-1 substrates with an expression pattern that coincides both temporally and spatially with ZIF-1 activity. Despite being ZIF-1 substrates, MEX-5/6 have been shown to be required for ZIF-1-dependent degradation through an unknown mechanism (DeRenzo et al., 2003). OMA-1 and -2, although containing tandem CCCH zinc fingers, are not degraded via a ZIF-1-dependent mechanism (DeRenzo et al., 2003; Detwiler et al., 2001).

In this study, we investigate spatial and temporal control of ZIF-1 expression in the early embryo. We show that the somatic cell-specific translation pattern of *zif-1* is a result of both net positive regulation in soma and repression in germline blastomeres. POS-1, MEX-3, and SPN-4 negatively regulate, whereas MEX-5 and MEX-6 positively regulate the expression of *zif-1*. All five proteins can bind to the *zif-1* 3′ UTR in vitro, suggesting direct regulation. POS-1, MEX-3, MEX-5, and MEX-6 share partially overlapping binding sites on the *zif-1* 3′ UTR and have antagonistic roles in *zif-1* expression. We propose that the precise combinatorial expression of these five RNA-binding proteins determines whether the *zif-1* transcript is translated in a particular blastomere.

Results

Nucleotides 64–123 of the zif-1 3′ UTR are required for repression in germline blastomeres and expression in somatic blastomeres

To investigate the mechanism by which the temporal and spatial expression pattern of *zif-1* is regulated in embryos, we performed deletion analyses of the *zif-1* 3′ UTR in vivo. The *zif-1* 3′ UTR (304 nucleotides) was arbitrarily divided into five approximately 60 nucleotide regions (I–V, Fig. 1B and Suppl Fig. S1; Guven-Ozkan et al., 2010). GFP::H2B reporters driven by the *zif-1* 3′ UTR with each of these five regions individually deleted were generated, and the expression pattern in transgenic embryos was analyzed. No change in GFP::H2B expression was detected with any of the *zif-1* 3′ UTR single region deletion reporters, with the exception of Region II deletion (ΔII), which lacks nucleotides 64–123 (Figs. 1C and E, $n>100$ for each transgene). This GFP reporter will be referred to as GFP::H2B$^{zif\text{-}1\Delta II}$. GFP::H2B$^{zif\text{-}1\Delta II}$ exhibited nuclear GFP in germline blastomeres P3 and P4, and no GFP in somatic blastomeres, a highly noteworthy expression pattern as it is reciprocal to what is observed in wildtype embryos (Figs. 1C and E, $n>200$). This result suggests (1) that somatic blastomere-specific expression of GFP::H2B$^{zif\text{-}1}$ is due to both negative regulation in germline blastomeres and positive regulation in somatic blastomeres, and (2) that Region II of the *zif-1* 3′ UTR mediates binding by both negative and positive regulators of ZIF-1 expression.

POS-1 represses and MEX-5/MEX-6 promote expression of zif-1, all via binding to nucleotides 64–123 of the zif-1 3′ UTR

To identify RNA-binding protein(s) that bind to *zif-1* 3′ UTR Region II and regulate spatial and temporal expression of ZIF-1, we directly tested RNA-binding proteins known to play key functional roles in early embryos, including POS-1, SPN-4, MEX-3, MEX-5, PIE-1, and MEX-1 (Draper et al., 1996; Guedes and Priess, 1997; Mello et al., 1992; Ogura et al., 2003; Schubert et al., 2000; Tabara et al., 1999). Biotinylated single-stranded *zif-1* 3′ UTR RNA was incubated with bacterially-expressed MBP-fused test proteins. RNA, along with associated proteins, was pulled down using streptavidin-conjugated magnetic beads. MBP-fused protein pulled down with the RNA was analyzed by western blots using an anti-MBP antibody. We found that POS-1, SPN-4, MEX-3, and MEX-5 all bound to the full-length *zif-1* 3′ UTR in a sense strand-specific manner (Figs. 1D and E, and data not shown). No specific binding was detected with PIE-1 or MEX-1 (data not shown). We also performed RNA pull-downs with RNAs corresponding to the *zif-1* 3′ UTR with the five arbitrarily-defined regions deleted, either individually or in combination. We observed that binding by both POS-1 and MEX-5 was dramatically reduced if RNA with Region II deleted was used in the pull down. Individual deletion of any other region had minor or no effect upon POS-1 or MEX-5 binding (Figs. 1D and E).

To determine whether POS-1 and/or MEX-5 regulate expression of ZIF-1, we depleted *pos-1*, or *mex-5* and *mex-6*, by RNAi in the transgenic strain expressing GFP::H2B$^{zif\text{-}1}$ (Fig. 2A). Depletion of *pos-1* by RNAi resulted in derepression of GFP::H2B$^{zif\text{-}1}$ in germline blastomeres, which can be detected, albeit weakly, as early as P2 (20% embryos scored positive, $n=40$), and clearly in P3 (100% embryos scored positive, $n=55$). MEX-5 and MEX-6 share high sequence similarity, exhibit identical expression patterns, and have partially redundant functions in vivo, which suggests that they are likely to bind to the same RNA targets. Simultaneous depletion of *mex-5* and *mex-6*, either by RNAi or genetic mutation [*mex-5(zu199);mex-6(pk440)*], resulted in a complete loss of GFP::H2B$^{zif\text{-}1}$ in embryos (100%, $n=120$ and 300, respectively). We also observed abnormal persistence of GFP::PIE-1 ZF1 in *mex-5/6(RNAi)* embryos (100%, $n=90$), and precocious degradation in *pos-1(RNAi)* embryos (100% embryos with a reduced GFP in P4, $n=166$) (Fig. 2A), phenotypes

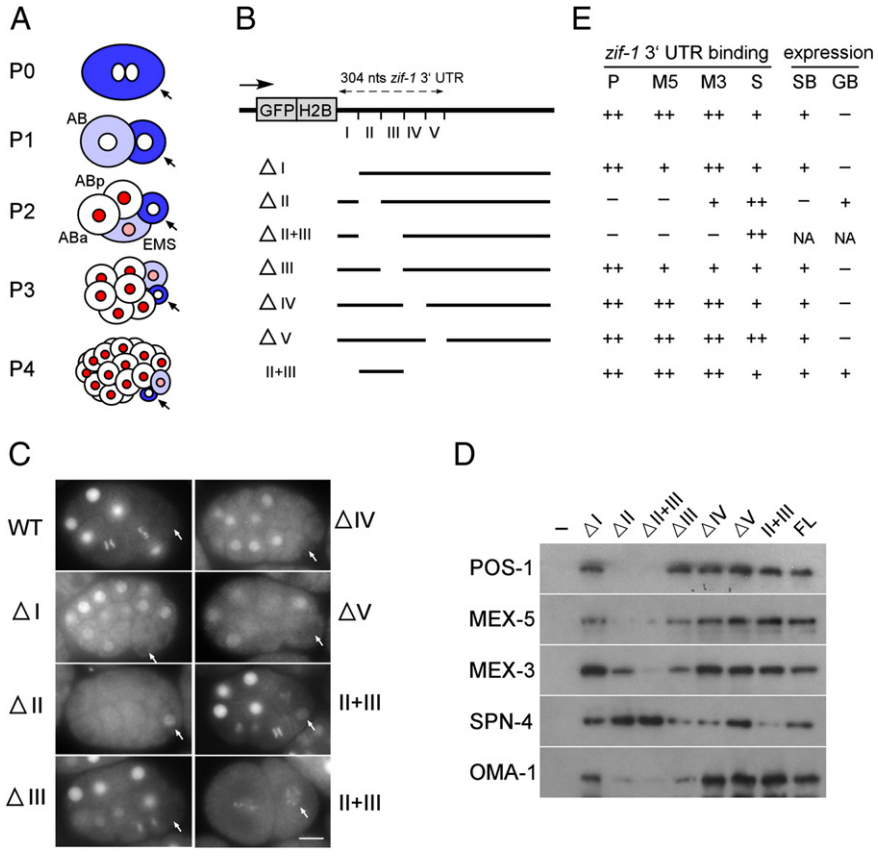

Fig. 1. In vitro and in vivo analyses show importance of nucleotides 64–123 of the *zif-1* 3′ UTR. (A) Sequential staging of early *C. elegans* embryos as determined by the P lineage blastomere (arrows). Blue: PIE-1 localization to the germline blastomere (dark blue), compared to its somatic sister (light blue). Red: expression of GFP::H2B^{zif-1}. Names of selected blastomeres are indicated. Arrows: germline blastomeres. (B) Schematic of the *zif-1* 3′ UTR, the five ~60 nt subregions, and the deletion constructs utilized. (C) Representative fluorescence micrographs of embryos expressing GFP::H2B reporters under the control of the indicated *zif-1* 3′ UTR. Bar: 10 μM. (D) In vitro RNA pulldowns using the indicated purified MBP-tagged protein and various forms of the *zif-1* 3′ UTR RNAs as shown in (B). After pulldown of RNA, protein bound to the RNA was assayed by Western blot using anti-MBP antibodies. The amount of SPN-4 pulled down appears to increase slightly with RNAs missing region II or V. We do not know the significance of this observation. FL: full length (304 nt). – : no RNA. (E) Summary of results in (C) and (D). P: POS-1; M5: MEX-5; M3: MEX-3; S: SPN-4; SB: somatic blastomere; GB: germline blastomere; NA: not analyzed due to derepression in oocytes.

previously reported for *mex-5/6(−)* and *pos-1(−)* mutant embryos (DeRenzo et al., 2003; Tabara et al., 1999). The phenotypes generated by either *pos-1(RNAi)* or *mex-5/6(RNAi)*, with respect to GFP::H2B^{zif-1} expression, are dependent on Region II of the *zif-1* 3′ UTR, as depletion of *pos-1* or *mex-5/6* resulted in no change in the expression of GFP::H2B$^{zif-1\Delta II}$ ($n>50$ for each RNAi, Fig. 2B). Taken together, these results support a model whereby POS-1 negatively regulates, and MEX-5/6 positively regulate, the expression of ZIF-1, both via direct binding to Region II of the *zif-1* 3′ UTR.

Depletion of *pos-1* or *mex-5/6* results in embryos with altered polarity, which could indirectly affect the expression of GFP::H2B^{zif-1}. Ideally, one would generate reporters with the *zif-1* 3′ UTR mutated for POS-1 binding sites or MEX-5 binding sites and assay their expression in embryos. The preferred binding sequences for the zinc fingers of POS-1 and MEX-5 in vitro have been investigated using electrophoretic mobility shift (EMSA) and fluorescence polarization (FP) assays (Farley et al., 2008; Pagano et al., 2007). Examination of the *zif-1* 3′ UTR identified four likely binding sites for POS-1 in Region II. However, three overlap with putative binding sites for MEX-5 (Fig. 2C and Suppl Fig. S1), precluding conclusive mutational analyses.

The overlapping putative POS-1 and MEX-5/6 binding sites within Region II of the *zif-1* 3′ UTR suggested that these proteins might have antagonistic functions in *zif-1* expression in cells where POS-1 and MEX-5/6 co-localize. We tested therefore whether POS-1 and MEX-5/6 binding to the *zif-1* 3′ UTR in vitro is antagonistic. The biotinylated *zif-1* 3′ UTR RNA efficiently pulled down POS-1 or MEX-5 in the in vitro binding assay when either protein was presented alone. However, when both MEX-5 and POS-1 were presented simultaneously, MEX-5 was preferentially pulled down at the expense of POS-1 (Fig. 2D). This result argues that MEX-5 binding to the *zif-1* 3′ UTR is preferred over POS-1 binding, and that MEX-5 binding impedes POS-1 binding. All together, our results support an antagonistic function between POS-1 and MEX-5 in the expression of ZIF-1 in vivo. In addition, they provide an explanation for how expression of MEX-5/6 could overcome the repressive function of POS-1 in somatic blastomeres newly separated from germline blastomeres.

Two distinct functions for MEX-5 and MEX-6 in promoting zif-1 translation in somatic blastomeres

In *mex-5(zu199);mex-6(pk440)* mutant embryos, many proteins that are normally localized to the germline blastomeres, such as POS-1, have been shown to be uniformly distributed throughout the embryo (Schubert et al., 2000). Uniform distribution of POS-1, a repressor for *zif-1* expression, could account for, or contribute to, the loss of GFP::H2B^{zif-1} expression in *mex-5(zu199);mex-6(pk440)* embryos. Indeed, depletion of *pos-1* by RNAi in *mex-5(zu199);mex-6(pk440)* embryos results in the expression of GFP::H2B^{zif-1} in all cells in embryos at the 4-cell stage and older (100%, $n>200$; Fig. 3). This result suggests that ectopic POS-1 accounts for most, if not all, of the loss of *zif-1* expression in *mex-5/6(−)* embryos. In addition, it suggests that MEX-5/6 are not absolutely required for ZIF-1 expression when POS-1 is absent. In wildtype embryos, MEX-5 and MEX-6 levels are low in germline blastomeres due to the germline-

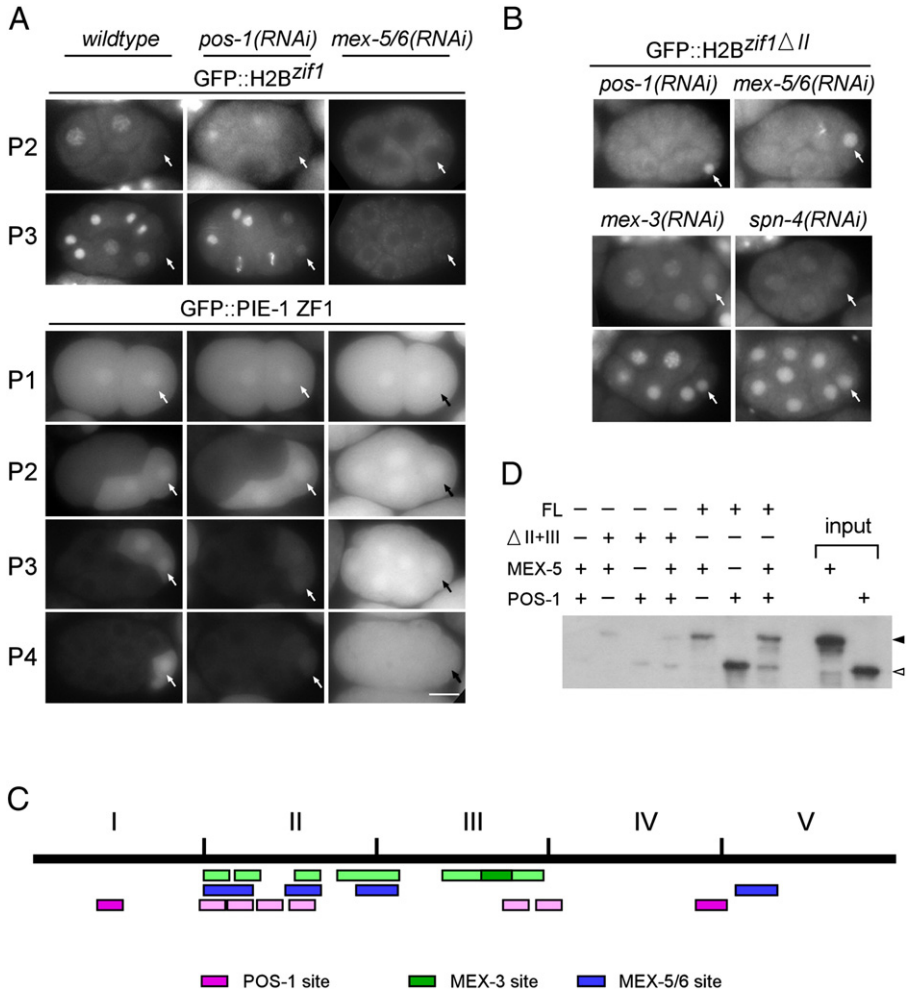

Fig. 2. POS-1, MEX-3, and SPN-4 repress whereas MEX-5/6 promote ZIF-1 expression in vivo. (A) Fluorescence micrographs of staged embryos, indicated on the left by the germline blastomere (arrows), expressing GFP::H2B^{zif-1} (top panels) or GFP::PIE-1 ZF1 (bottom panels) in wildtype, *pos-1(RNAi)*, and *mex-5/6(RNAi)* backgrounds. Bar: 10 μM. (B) Embryos expressing GFP::H2B$^{zif-1\Delta II}$ in *pos-1(RNAi)*, *mex-5/6(RNAi)*, *mex-3(RNAi)*, and *spn-4(RNAi)* backgrounds. Both 4-cell and 8-cell embryos are shown for *mex-3(RNAi)*, and *spn-4(RNAi)*. (C) Schematic of putative binding sites for POS-1 (pink, 5′ UAU$_{2-3}$RDN$_{1-3}$G 3′), MEX-3 (green, 5′ (A/G/U)(G/U)AGN(0–8)U(U/A/C)UA 3′) and MEX-5/6 (blue, minimum 6 U per 8-nucleotide stretch) on the five regions of the *zif-1* 3′ UTR (Farley et al., 2008; Pagano et al., 2009; Pagano et al., 2007). Sequences that deviate by one nucleotide from the published optimal POS-1- and MEX-3-binding sites are indicated in lighter pink and lighter green, respectively. (D) POS-1 and MEX-5/6 binding to the *zif-1* 3′ UTR in vitro is antagonistic. In vitro RNA pulldowns using MEX-5 (arrow head), POS-1 (open arrowhead), or both, and indicated forms of the *zif-1* 3′ UTR RNAs were performed as in Fig. 1D.

blastomere-specific serine/threonine kinase, PAR-1. In *par-1(RNAi)* embryos, MEX-5 and MEX-6 are present at high levels in all early blastomeres (Schubert et al., 2000), and ZIF-1-dependent degradation of CCCH finger-containing proteins is detected in all cells (DeRenzo et al., 2003). We observed uniform distribution of GFP::H2B^{zif-1} in *par-1(RNAi)* embryos that is dependent on MEX-5/6 activity. While GFP::H2B^{zif-1} is not expressed in *par-1(RNAi); mex-5(RNAi)* embryos (0%, n > 200), it is expressed when *pos-1* is also depleted (100% embryos 4-cell and older, n > 200; Fig. 3). Taken together, our results demonstrate two distinct functions for MEX-5 and MEX-6 as positive regulators of *zif-1* expression. First, MEX-5 and MEX-6 restrict the repressor POS-1 to germline blastomeres, releasing repression in somatic blastomeres. Second, in cells where MEX-5, MEX-6, and POS-1 co-localize, MEX-5/6 compete with POS-1 for overlapping binding sites on the *zif-1* 3′ UTR, antagonizing a POS-1 repressive effect.

MEX-3 and SPN-4 bind to the zif-1 3′ UTR and repress zif-1 translation in embryos

The above results demonstrate that MEX-5/6 are not absolutely required for the expression of *zif-1* in somatic blastomeres. However, a GFP reporter regulated by the *zif-1* 3′ UTR lacking Region II (GFP::H2B$^{zif-1\Delta II}$), and therefore independent of POS-1 and MEX-5/6 regulation (Figs. 1C and 2B), is nonetheless repressed in somatic blastomeres. This observation suggests one or more additional RNA-binding proteins that repress expression of *zif-1* in somatic blastomeres through regions outside of Region II in the 3′ UTR. Because POS-1 accounts for most, if not all repression in *mex-5(zu199);mex-6(pk440)* embryos, this hypothetical RNA binding protein(s) is expected to be absent or inactive in *mex-5(zu199);mex-6(pk440)* embryos. Indeed, through RNA pulldown experiments we have identified two other proteins that exhibit specific binding to the *zif-1* 3′ UTR: MEX-3 and SPN-4 (Figs. 1D and E). MEX-3 binds to Regions II and III of the *zif-1* 3′ UTR. Deleting Region II or III alone results in a modest reduction whereas deleting both Region II and III results in a dramatic reduction in MEX-3 binding to the *zif-1* 3′ UTR. It has been shown previously that MEX-3 expression is abolished in *mex-5(zu199);mex-6(pk440)* mutant embryos (Schubert et al., 2000), making it a likely candidate for this predicted RNA-binding protein. SPN-4, on the other hand, although demonstrating *zif-1* 3′ UTR sense strand specificity, exhibited less sequence-specificity in its binding. SPN-4 binding was reduced, but not abolished, after pulldown of RNAs corresponding to the *zif-1* 3′ UTR deleted of either regions III or IV. Most dramatically, depletion of either *mex-3* or

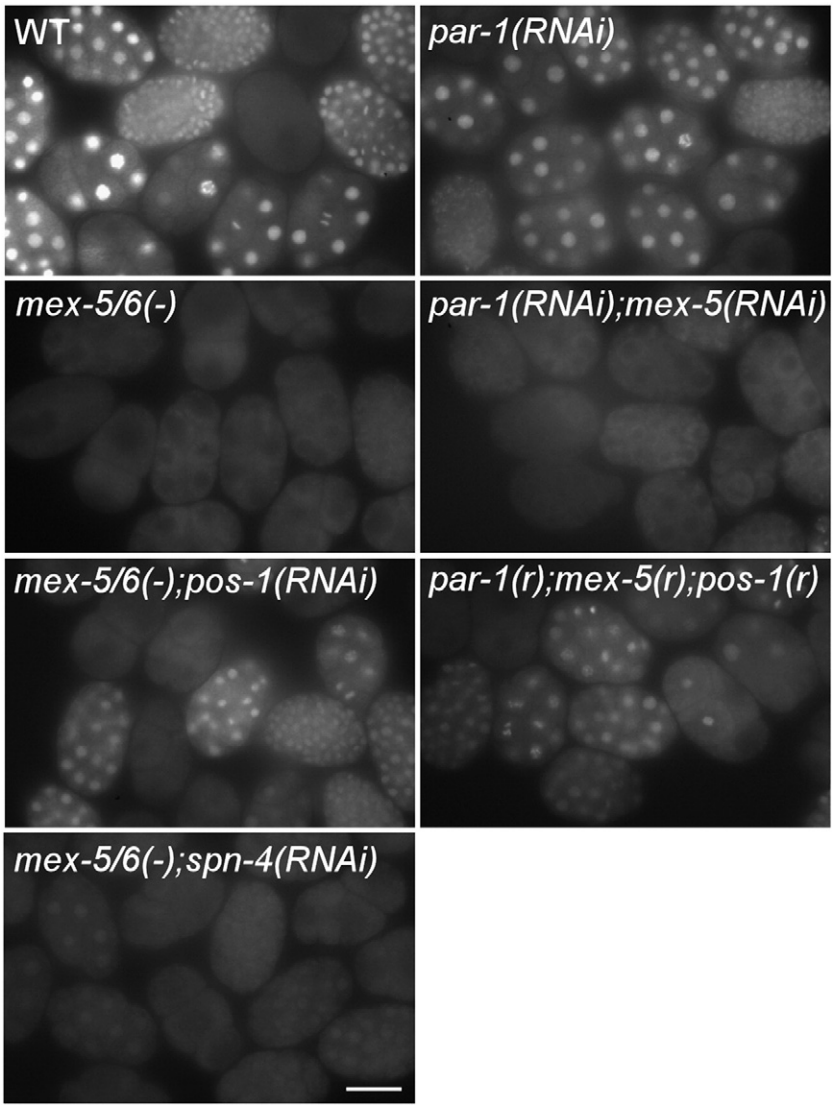

Fig. 3. MEX-5/6 positively regulate *zif-1* expression in embryos by antagonizing repression by POS-1. Fluorescence micrographs of groups of embryos expressing GFP::H2B$^{zif\text{-}1}$ in the indicated genetic backgrounds. Depletion of *pos-1* suppresses the GFP::H2B$^{zif\text{-}1}$ defect in *mex-5(zu199);mex-6(pk440)* [*mex-5/6(−)*] and *par-1(RNAi);mex-5(RNAi)* embryos. In the bottom right hand panel, (RNAi) was abbreviated to (r) due to space limitation. Bar: 30 μM.

spn-4 resulted in uniform expression of GFP::H2B$^{zif\text{-}1\Delta II}$ in all cells as early as in the 4-cell stage (100% embryos 4-cell and older, n > 100 for each RNAi; Fig. 2B). These results together support the model that MEX-3 and SPN-4 repress expression of ZIF-1, also by direct binding to the *zif-1* 3′ UTR.

The preferred RNA sequence in vitro for the MEX-3 RNA-binding domain has also been determined (Pagano et al., 2009). Analysis of the *zif-1* 3′ UTR revealed many possible MEX-3 binding sites, all within Regions II and III, that also overlap putative binding sites for POS-1, MEX-5, or both (Fig. 2C and Suppl. Fig. S1). Consistent with their partially overlapping binding sites, we could show that MEX-3 and MEX-5/6 function antagonistically in regulating *zif-1* expression in vivo. Embryos depleted of *mex-5* alone exhibit a reduction in GFP::H2B$^{zif\text{-}1}$ expression (Fig. 4). This reduction can be suppressed when *mex-3* is simultaneously depleted. With *mex-6(RNAi)*, which resulted in a mild reduction in GFP::H2B$^{zif\text{-}1}$ expression, a similar suppression was observed. In fact, depletion of *mex-3* in wildtype or *par-1(RNAi)* embryos resulted in a detectable increase in overall levels of GFP::H2B$^{zif\text{-}1}$. Depletion of *mex-3* did not suppress *mex-5(zu199);mex-6(pk440)* embryos where MEX-3 is already low or absent (Fig. 4).

MEX-3 and SPN-4 function together in repressing ZIF-1 expression

The result that depletion of either *mex-3* or *spn-4* resulted in a uniform expression of GFP::H2B$^{zif\text{-}1\Delta II}$ in all cells as early as the 4-cell stage (Fig. 2B) was somewhat unexpected, as SPN-4 has always been considered germline blastomere-enriched, and MEX-3 somatic blastomere-enriched (Draper et al., 1996; Ogura et al., 2003). Both SPN-4 and MEX-3 proteins are present at high levels in 1-cell embryos. At each germline blastomere division, SPN-4 protein is initially equal between the two daughters, but is then degraded only in the somatic daughters (Supplemental Figs. S2 and S3) (Ogura et al., 2003). MEX-3, on the other hand, is enriched in AB after the first mitotic division. Low levels of MEX-3 remain in germline blastomeres where it, like many RNA-binding proteins identified in germline blastomeres, associates with germline specific P-granules. The uniform expression of GFP::H2B$^{zif\text{-}1\Delta II}$ in *spn-4(RNAi)* and *mex-3(RNAi)* embryos, combined with asymmetric localization of both SPN-4 and MEX-3 after the 2-cell stage, suggests a repressive function for both SPN-4 and MEX-3 in 1- or 2-cell stage embryos.

Consistent with the above possibility, depletion of *spn-4* in wildtype embryos by RNAi resulted in the detection of GFP::H2B$^{zif\text{-}1}$ in P2 and

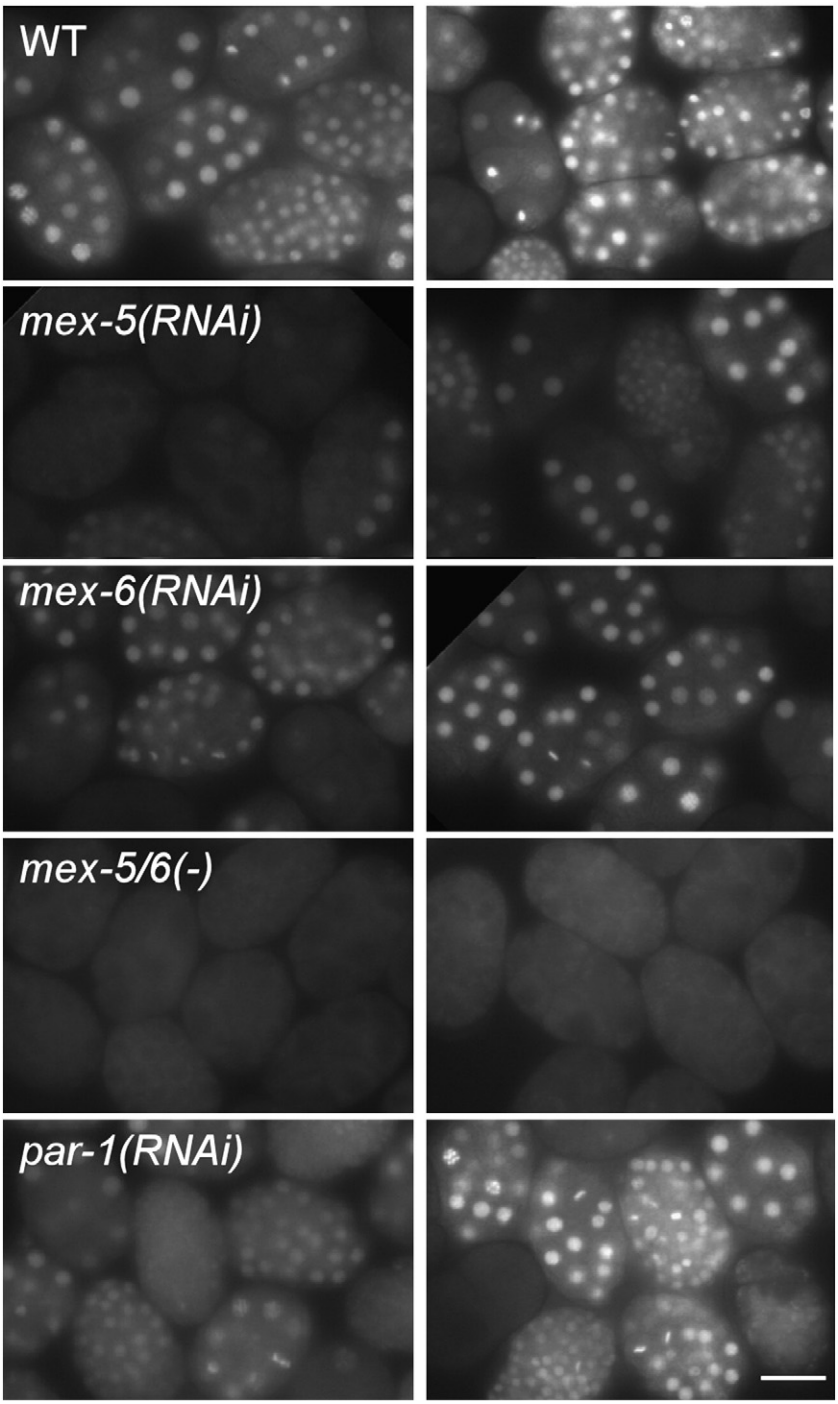

Fig. 4. MEX-3 represses *zif-1* expression. Fluorescence micrographs of GFP::H2B$^{zif\text{-}1}$ expression in groups of embryos depleted of various proteins (indicated in left column). Each row compares GFP::H2B$^{zif\text{-}1}$ intensities in the indicated genetic backgrounds between *mex-3* depletion (right) or nondepletion (left). Depletion of *mex-3* increases GFP signal except in the *mex-5(zu199);mex-6(pk440)* [*mex-5/6(−)*] background which expresses little or no MEX-3 protein. Bar: 30 μM.

EMS of very young 4-cell embryos (100%, n = 120, Fig. 5A). GFP::H2B$^{zif\text{-}1}$ can also be detected in both P2 and EMS of early 4-cell embryos derived from *mex-3(zu155)* mutant worms (100%, n = 40). For *mex-3(zu155)* worms that are also depleted of *spn-4* by RNAi, GFP::H2B$^{zif\text{-}1}$ signal can be detected, albeit weakly, as early as 2-cell embryos (10%, n = 50). Further supporting the early repressive function of SPN-4, we showed that a GFP::H2B reporter regulated by only Regions II and III of the *zif-1* 3′ UTR (GFP::H2B$^{zif\text{-}1\ II+III}$), a region not bound by SPN-4 in our in vitro binding assay (Figs. 1D and E), is properly repressed in oocytes, where repression is OMA-1/2-dependent (Guven-Ozkan et al., 2010), but uniformly expressed in embryos as early as the 2-cell stage (Fig. 1C).

MEX-3 and SPN-4 have been shown to bind each other in a yeast 2-hybrid assay (Huang et al., 2002). Two lines of evidence support a model that these two proteins function together in regulating *zif-1* expression. First, neither SPN-4 nor MEX-3 appears to be sufficient on its own for the translational repression of *zif-1*, as shown by the following three examples. (1) Depletion of *pos-1* results in derepression of *zif-1* in germline blastomeres, despite a high level of SPN-4 (and low MEX-3) (Fig. 2A). (2) SPN-4, like POS-1, is uniformly distributed in *mex-5(zu199);mex-6(pk440)* embryos (100%, n = 40; Supplemental Fig. S2), a genetic background where MEX-3 protein is absent (Schubert et al., 2000). However, POS-1, but not SPN-4, is responsible for the *zif-1*

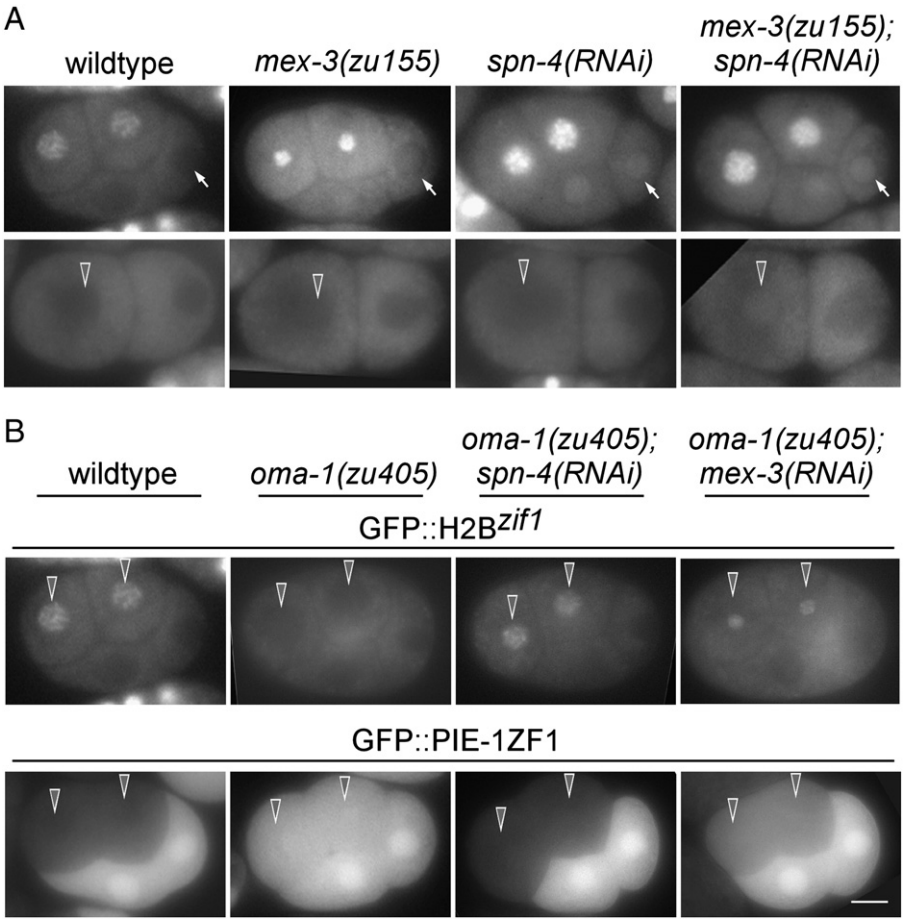

Fig. 5. MEX-3 and SPN-4 function together to repress *zif-1* expression. (A) Fluorescence micrographs of GFP::H2B^{zif-1} expression in 2-cell and 4-cell wildtype, *mex-3(zu155)*, *spn-4(RNAi)*, or *mex-3(zu155);spn-4(RNAi)* embryos. GFP::H2B^{zif-1} signal can be detected in all blastomeres in early 4-cell embryos upon depletion of *mex-3*, *spn-4*, or both. GFP was detected in some 2-cell embryos depleted of both genes. (B) Fluorescence micrographs of 4-cell embryos expressing GFP::H2B^{zif-1} or GFP::PIE-1 ZF1 in the indicated genetic backgrounds. GFP::H2B^{zif-1} expression in somatic blastomeres (arrows) is ectopically repressed in *oma-1 (zu405)* embryos. The GFP::H2B^{zif-1} defect in *oma-1(zu405)* is suppressed when *mex-3* or *spn-4* is depleted. A reciprocal pattern is seen in embryos carrying GFP::PIE-1 ZF1. Bar: 10 μM.

repression in *mex-5(zu199);mex-6(pk440)* embryos. Depletion of *pos-1*, but not *spn-4*, restored GFP::H2B^{zif-1} expression in *mex-5(zu199);mex-6(pk440)* embryos (Fig. 3). (3) Similarly, we observed no ectopic repression of GFP::H2B^{zif-1} in *spn-4(RNAi)* embryos (data not shown), which have been shown to maintain high MEX-3 levels in all blastomeres until approximately the 28-cell stage (Huang et al., 2002). The second line of evidence supporting SPN-4 and MEX-3 acting together comes from analysis in the *oma-1(zu405)* genetic background. We showed previously that the *oma-1(zu405)* missense mutation results in OMA-1 protein persisting past the 1-cell stage and repressing translation of *zif-1* in somatic blastomeres (Guven-Ozkan et al., 2010; Nishi and Lin, 2005). The ectopic *zif-1* repression in *oma-1(zu405)* embryos is most apparent in 4-cell embryos, and progressively lessens in older embryos (Guven-Ozkan et al., 2010). Degradation of many maternally-supplied proteins is also defective in *oma-1(zu405)* embryos, including MEX-5/6, POS-1, MEX-3, and SPN-4 (Lin, 2003) and Supplemental Fig. S3). We find that depletion of *mex-3* or *spn-4*, but not *pos-1* or *mex-5/6*, partially suppresses the ectopic repression of *zif-1* (40%, n = 20 for *mex-3(RNAi)* and 70%, n = 20 for *spn-4(RNAi)*) and degradation of GFP::PIE-1 ZF1 in *oma-1(zu405)* embryos (50%, n = 50 for *mex-3(RNAi)* and 85%, n = 50 for *spn-4(RNAi)*; Figs. 5B and Supplemental Fig. S4).

Expression of zif-1 in newly formed somatic cells requires high MEX-5/6 and low MEX-3 levels

One interesting question that remains is how *zif-1* expression is turned on in somatic daughters (EMS, C, and D) newly divided from a germline blastomere where *zif-1* is actively repressed. Although POS-1 and SPN-4 are germline-enriched proteins, their levels are initially equal and high between newly formed somatic cells and their sister germline blastomeres (Ogura et al., 2003; Tabara et al., 1999). Therefore, initiation of *zif-1* expression cannot be explained by the asymmetric localization of its repressors, POS-1 and SPN-4. The levels of MEX-5/6, the positive regulators of *zif-1* expression, are coincidently increased in all newly formed somatic blastomeres (Schubert et al., 2000). Because MEX-5/6 antagonizes repression by POS-1, it is possible that an increase in MEX-5/6 levels is sufficient to allow *zif-1* expression in these newly-formed somatic blastomeres. In addition, we considered whether two other factors contribute to the initiation of *zif-1* expression in newly formed somatic cells. First, levels of MEX-3 protein, which negatively regulates *zif-1* expression and is a likely cofactor for SPN-4, are low in newly formed somatic blastomeres (Draper et al., 1996), and this might be important to relieve repression. Second, degradation of POS-1, which is both a substrate of ZIF-1 as well as a repressor of *zif-1* expression, could initiate a positive feedback loop that facilitates *zif-1* expression to high levels. SPN-4 is subsequently degraded by a yet unknown mechanism.

If a low level of MEX-3 protein is critical for the onset of translation of *zif-1*, then in embryos in which MEX-3 is ectopically expressed in the EMS lineage, GFP::H2B^{zif-1} expression should be decreased or abolished. The *med-1* promoter has been shown to drive GFP-fused transgenic proteins specifically in the EMS lineage (Maduro et al., 2001). We were unable to use two different fluorescent tags for this experiment for technical reasons: H2B^{zif-1} tagged with mCherry

exhibited slower maturation and degradation than GFP and we were unable to recover mCherry::MEX-3 expressing lines for unknown reasons. However, because MEX-3 is expressed exclusively in the cytoplasm (Fig. 6A) and GFP::H2B^{zif-1} is primarily nuclear, we were able to assay the effect on GFP::H2B^{zif-1} expression by confocal microscopy of embryos also expressing cytoplasmic GFP::MEX-3. In addition, cytoplasmic GFP::MEX-3 is degraded very rapidly and is mostly undetectable in 28-cell stage embryos, the stage at which we analyzed the effect on nuclear GFP::H2B^{zif-1} expression (Fig. 6A). At the 28-cell stage, there are six blastomeres derived from the EMS blastomere, four from MS and two from E blastomeres. We measured nuclear GFP signal in the EMS descendants and AB descendants on the same focal planes. Nuclear GFP signal in the four MS descendants and two E descendants is presented as a ratio to the nuclear GFP signal in the AB blastomeres of the same embryo. Nuclear GFP in EMS descendants is significantly lower in embryos expressing ectopic GFP::MEX-3 than embryos without ectopic GFP::MEX-3 (Figs. 6A and B). This supports the model that a low level of MEX-3 protein in newly formed somatic blastomeres is important to relieve *zif-1* translational repression.

To test whether degradation of POS-1 in EMS is required for translation of *zif-1* in EMS, we depleted *zif-1* by RNAi and assayed the onset of GFP::H2B^{zif-1} signal in EMS compared to that in nonRNAi embryos. We also depleted *zif-1* in the strain expressing GFP::PIE-1 ZF1 in a parallel experiment as a control to monitor the effect of *zif-1(RNAi)* on the degradation of ZIF-1 targets. *zif-1(RNAi)* resulted in a defect in the degradation of, and therefore uniform distribution of, GFP::PIE-1 ZF1 in embryos up to at least the 20-cell stage (100%, n > 100). Despite successful inhibition of GFP::PIE-1 ZF1 degradation, we observed no difference in the timing of onset of expression for GFP::H2B^{zif-1} in the EMS lineage (0%, n = 30; Fig. 6C). This result suggests that degradation of POS-1 is not important for translation of *zif-1* in EMS.

Discussion

Spatial and temporal restriction of ZIF-1 expression exclusively to somatic blastomeres is critical to achieve localization of PIE-1 specifically to germline blastomeres. We show here that the combination of both repression in germline blastomeres and activation in somatic blastomeres results in somatic cell-specific expression of *zif-1*. Multiple RNA-binding proteins, which individually can either activate or repress *zif-1* expression via direct binding to the *zif-1* 3′ UTR, function in a combinatorial fashion to effect either net repression or net activation of *zif-1* translation. Many of these RNA-binding proteins physically interact with one another as well as compete for the same or overlapping binding sites (Fig. 7). As *zif-1* RNA is maternally supplied and uniformly distributed in early embryos (http://nematode.lab.nig.ac.jp/db2/ShowCloneInfo.php?clone=570e9), we believe that the effect on ZIF-1 expression by these RNA-binding proteins is primarily through translational regulation.

We show that POS-1, SPN-4, and MEX-3 all repress expression of the *zif-1* reporter (Fig. 7). MEX-3 and SPN-4 have been shown to physically interact (Huang et al., 2002). Our results that both MEX-3 and SPN-4 are required for complete repression of ZIF-1 expression support a model that they function together to effect *zif-1* repression. However, we cannot rule out the possibility that MEX-3 and SPN-4 function in parallel pathways. It is possible that physical binding between these two proteins stabilizes their binding to target RNA(s). Further biochemical analyses will be needed to address this possibility. We propose that wherever MEX-3 and SPN-4 co-localize, such as P0, they repress translation of *zif-1*. After the first division, both MEX-3 and SPN-4 are initially present at high levels in both daughters (Draper et al., 1996; Ogura et al., 2003). Therefore, *zif-1* continues to be repressed in both blastomeres. Translational repression of *zif-1* in AB is lifted following degradation of SPN-4 later in the cell cycle through an unidentified mechanism, which results in ready detection of *zif-1* translational reporters in ABa and ABp. Meanwhile, MEX-3 decreases in level in P1, and becomes primarily localized to the germline P-granules. We do not believe that the MEX-3 in P-granules functions in conjunction with SPN-4 to repress ZIF-1 expression, as depletion of POS-1 resulted in the derepression of the *zif-1* transgene in later germline blastomeres where SPN-4 and P-granule-bound MEX-3 are present (Draper et al., 1996; Ogura et al., 2003). It is often observed that the detection of reporter GFP is delayed by one cell cycle

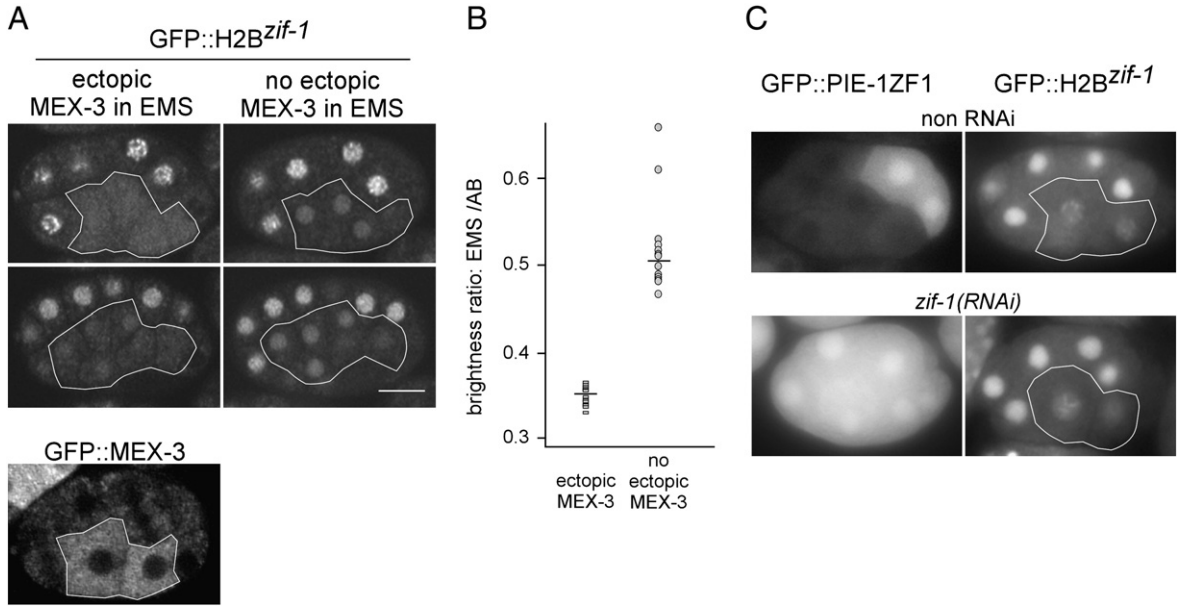

Fig. 6. Low MEX-3 levels are important for *zif-1* expression in newly-formed somatic cells. (A) Top two rows: confocal microscopy images of embryos expressing GFP::H2B^{zif-1} with (left column) or without (right column) ectopic GFP::MEX-3 in the EMS lineage descendents (outlined). Top row: 16-cell stage. Second row: the same embryos at 28-cell stage. The bottom panel shows the exclusive cytoplasmic signal from GFP::MEX-3 in a 12-cell embryo without GFP::H2B^{zif-1}. (B) Quantification of GFP::H2B^{zif-1} signal in embryos with or without GFP::MEX-3 in the EMS lineage of 28-cell embryos. Y axis represents the ratio of average nuclear GFP intensity in the EMS lineage to that in the AB lineage in individual embryos. Thirteen embryos of each genotype were scored. −− = mean. (C) Fluorescence micrographs of embryos expressing GFP::PIE-1 ZF1 (left column) or GFP::H2B^{zif-1} (right column) in wildtype and *zif-1(RNAi)* backgrounds. The onset of GFP::H2B^{zif-1} expression remains unchanged upon *zif-1(RNAi)*. Bar:10 μM.

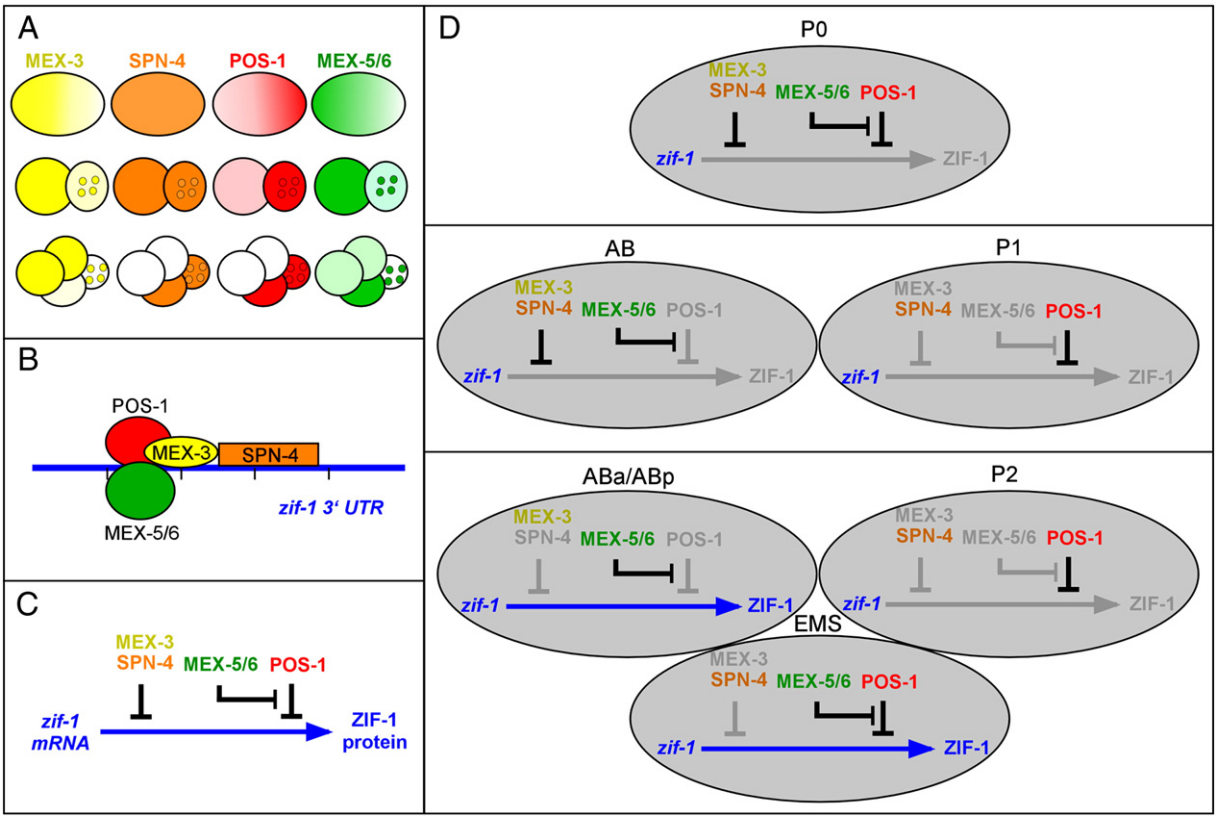

Fig. 7. Model. Schematic representation showing (A) endogenous expression patterns of MEX-3 (yellow), SPN-4 (orange), POS-1 (red), and MEX-5/6 (green) in 1-, 2- and 4-cell embryos, (B) the deduced binding sites on the *zif-1* 3′ UTR for MEX-3, SPN-4, POS-1, and MEX-5/6 based on our RNA-binding assays, and (C) the proposed effects of these RNA-binding factors on *zif-1* translation. (D) Proposed regulation of *zif-1* translation in each early blastomere, as a result of the combinatorial effects of MEX-3, SPN-4, POS-1, and MEX-5/6, resulting from the dynamic temporal and spatial localization of each protein. Gray arrow: no ZIF-1 expression; blue arrow: ZIF-1 expression. See text for details.

compared to the onset of expression of the endogenous protein. Therefore we suggest that continued repression of *zif-1* in the P lineage is maintained by the function of POS-1, most likely beginning with the P2 blastomere. Our finding that POS-1 and MEX-3 repress translation of *zif-1* is consistent with previous findings that reduced levels of PIE-1, and therefore derepression of zygotic transcription, were detected in P4 blastomeres of both *pos-1(−)* and *mex-3(−)* mutant embryos (Tabara et al., 1999; Tenenhaus et al., 1998).

In EMS, the somatic daughter of the germline blastomere P1, levels of the translational repressors POS-1 and SPN-4 are initially high but *zif-1* is nonetheless translated. We find that translation of *zif-1* results from the combination of low levels of MEX-3, without which SPN-4 does not repress, along with a high level of activators MEX-5 and MEX-6, which antagonize repression by POS-1 (see below). Ectopic expression of MEX-3 in EMS, where SPN-4 levels are high, is sufficient to prevent or delay *zif-1* translation.

Translation of *zif-1* in somatic blastomeres requires MEX-5 and MEX-6. We show that MEX-5/6 have dual roles in promoting translation of *zif-1* in somatic blastomeres. First, they restrict POS-1, along with several other proteins, to germline blastomeres through their function in maintaining embryonic polarity (Schubert et al., 2000). Second, they bind to the *zif-1* 3′ UTR, enabling its translation. However, binding of MEX-5/6 to the *zif-1* 3′ UTR is not absolutely required for ZIF-1 translation, as evidenced by ZIF-1 expression in *pos-1;mex-5;mex-6* embryos. Instead, MEX-5/6 binding to the *zif-1* 3′ UTR enables ZIF-1 expression by preventing binding of repressors to the same region. This model is supported by the extensive overlap of MEX-5/6 and POS-1 binding sites in Region II, and that MEX-5 binding impedes POS-1 binding to the *zif-1* 3′ UTR in our in vitro assay. The antagonistic functions between MEX-5/6 and POS-1 are consistent with previous genetic analyses showing that a reduced dosage of *pos-1* suppresses the *mex-5* mutant phenotype (Tenlen et al., 2006). Our results here present a molecular mechanism for the requirement for MEX-5/6 in ZIF-1-mediated target protein degradation (DeRenzo et al., 2003). Furthermore, these results explain how MEX-5/6 can be expressed at a high level in cells where ZIF-1 degrading activity is also high, and how MEX-5/6 promote ZIF-1 degrading activity while simultaneously being substrates of ZIF-1 themselves (DeRenzo et al., 2003).

The region of the *zif-1* 3′ UTR bound by MEX-5/6 also partially overlaps with the binding sites for MEX-3 and OMA-1/2, three other key repressors of *zif-1* translation (Fig. 7B) (Guven-Ozkan et al., 2010; Pagano et al., 2009). We find that MEX-5/6 also antagonize repression of *zif-1* by MEX-3 and OMA-1/2 (M. O. and R. L., unpublished data). We did not, however, observe a clear competitive advantage for MEX-5 binding over MEX-3 binding in our in vitro pull down assay (M. O. and R. L., unpublished data). It is possible that the mechanism by which MEX-5/6 antagonize repression by MEX-3 is different from that utilized against POS-1. MEX-5/6 bind to MEX-3 in a yeast 2-hybrid assay (Huang et al., 2002). Therefore, MEX-5/6 could antagonize translational repression by MEX-3 through a protein–protein interaction, preventing MEX-3 from binding to the *zif-1* 3′ UTR. In cells where activators MEX-5/6 and their competing repressors, POS-1, MEX-3, or OMA-1/2 co-localize, the outcome regarding *zif-1* translation will likely be determined by the relative abundance of MEX-5/6 and their competing repressors.

POS-1 is both a repressor of *zif-1* translation as well as a target of ZIF-1-mediated degradation. This suggests that a positive feedback loop, whereby degradation of some POS-1 leads to further relief from POS-1-mediated repression, could accelerate the relief from translational repression of zif-1 by POS-1 in newly formed somatic sisters of P lineage blastomeres. However, we detected no difference in the expression of GFP::H2B$^{zif\text{-}1}$ when *zif-1* was depleted by RNAi, suggesting that such a positive feedback loop does not play a major role in the onset of *zif-1*

translation in EMS. It is likely that the level of MEX-5/6 in EMS is already sufficiently higher than that of POS-1 such that any further reduction of POS-1 levels would be inconsequential for the onset of *zif-1* translation. MEX-5/6 are themselves also targets of ZIF-1 degradation (DeRenzo et al., 2003), suggesting a possible negative feedback loop for *zif-1* translation which would limit the duration of ZIF-1 translation in somatic blastomeres. The effect of *zif-1* RNAi on the onset of GFP::H2B$^{zif\text{-}1}$ expression might therefore be compounded by the simultaneous inhibition of both positive and negative feedback loops.

Transcriptional repression is critical for maintaining both the stability and the totipotency of the germline. Proper development of the germline is, therefore, one of the most critical processes to occur during *C. elegans* early embryogenesis. However, the mechanism that has evolved to segregate PIE-1 to the germline precursors is not 100% effective, and some PIE-1 remains in the somatic sisters following division (Reese et al., 2000). Cell cycles last only 10–15 min in early *C. elegans* embryos (Seydoux and Fire, 1994), therefore any residual PIE-1 in somatic cells would interfere with the rapid onset of zygotic transcription that is crucial for somatic development. Asymmetric translation of ZIF-1 in somatic blastomere ensures rapid degradation of PIE-1 in somatic blastomeres.

To have so many RNA-binding factors, acting both positively and negatively, regulating the translation of *zif-1* simply to establish a somatic cell-specific translation pattern might seem to be overly complicated. Particularly counterintuitive is the discovery that *zif-1* expression is repressed by MEX-3, a protein enriched in somatic cells where *zif-1* is ultimately expressed. We suggest that *C. elegans* embryos are faced with a particularly unique challenge due to two aspects of their developmental program: (1) the way in which their germ cell precursors are specified (Strome and Lehmann, 2007), and (2) the fact that many maternally-supplied proteins, including almost all key RNA-binding proteins, are already translated prior to fertilization. It makes good sense for worms to utilize the germline blastomere-specific protein, POS-1, to repress the translation of *zif-1* in germline blastomeres, and somatic blastomere-specific proteins, MEX-5 and MEX-6, to compete with POS-1 and promote translation in newly formed somatic blastomeres. However, POS-1 and MEX-5/6 are all maternally-supplied proteins and are all present at a high level in the 1-cell embryo, P0, before being asymmetrically segregated to germline and somatic blastomeres, respectively. P0, like the other P lineage blastomeres, is a precursor for both somatic and germline blastomeres. High levels of POS-1, MEX-5, and MEX-6 in P0 would be predicted to promote the translation of *zif-1*, leading to precocious degradation of PIE-1 and embryonic lethality. *C. elegans* circumvents this dilemma by utilizing two additional RNA-binding proteins, SPN-4 and MEX-3, whose expression patterns only overlap in the 1-cell and 2-cell embryos, to function together to repress *zif-1* translation in 1- and 2-cell embryos. After the 2-cell stage, repression by SPN-4 and MEX-3 is relieved, and germline versus somatic regulation of ZIF-1 expression initiates. Repression in germline blastomeres is continued by the germline protein POS-1, and embryos only need to control *zif-1* translation in newly-formed somatic blastomeres.

We propose that multiple RNA-binding proteins, expressed in individual dynamic temporal and spatial patterns, function in a combinatorial manner to prevent the precocious translation of *zif-1*, localizing ZIF-1 activity strictly to the somatic blastomeres. Such regulation is essential for the stability of PIE-1 in germline blastomeres, global transcriptional repression in the germline precursors, and ultimately the maintenance of germline integrity and totipotency.

Experimental procedures

Strains

N2 was used as the wildtype strain. Genetic markers are: LGII, *mex-6 (pk440)*; LGIII, *unc-119(ed3)*; LGIV, *oma-1(zu405)*, *oma-1(zu405,te33)*, *mex-5 (zu199)*; and LGV, *oma-2(te51)*. Plasmids used, strain names and transgenes are as follows: TX1246 (*teIs113 [P$_{pie\text{-}1}$gfp::h2b::UTR$^{zif\text{-}1,771bp}$]*), TX1251 (*teIs604 [P$_{pie\text{-}1}$gfp::h2b::UTR$^{zif\text{-}1,771bp,\Delta 4\text{-}63}$]*), TX1288 (*oma-1(zu405; te33)/nT1; oma-2(te51)/nT1; teIs114 [P$_{pie\text{-}1}$gfp::h2b:: UTR-$^{zif\text{-}1,771bp}$]*), TX1298 (*teEx607 [P$_{pie\text{-}1}$gfp::h2b::UTR$^{zif\text{-}1,771bp,\ \Delta 184\text{-}243}$]*), TX1311 (*teEx610 [P$_{pie\text{-}1}$gfp::h2b::UTR$^{zif\text{-}1,771bp,\ 64\text{–}183}$]*), TX1481 (*mex-6(pk440); unc-30(e191)mex-5(zu199)/nT1; teIs113 [P$_{pie\text{-}1}$gfp::h2b:: UTR-$^{zif\text{-}1,771bp}$]*), TX1513 (*mex-6(pk440); unc-30(e191)mex-5(zu199)/nT1; axEx1120 [P$_{pie\text{-}1}$gfp::pie-1 zf1::UTR$^{pie\text{-}1}$, pRF4]*), TX1533 (*teIs140 [P$_{pie\text{-}1}$gfp::h2b::UTR$^{zif\text{-}1,771bp,\ \Delta 64\text{-}123}$]*), TX1541 (*teIs143 [P$_{pie\text{-}1}$gfp::h2b::UTR$^{zif\text{-}1,771bp,\ \Delta 114\text{-}183}$]*), TX1543 (*teIs145 [P$_{pie\text{-}1}$gfp::h2b::UTR$^{zif\text{-}1,771bp,\ \Delta 64\text{-}183}$]*), TX1567 (*teEx719 [P$_{med\text{-}1}$gfp::mex-3]*), TX1570 (*teIs113 [P$_{pie\text{-}1}$gfp::h2b:: UTR$^{zif\text{-}1,771bp}$]; teEx719 [P$_{med\text{-}1}$gfp::mex-3]*), JH1436 (*axEx1120 [Ppie-1gfp::pie-1 zf1::UTR$^{pie\text{-}1}$, pRF4]*).

Plasmid construction

Most plasmids were constructed with the Gateway cloning technology as previously described (Guven-Ozkan et al., 2010). The in vivo 3′ UTR functional assays used the 771 nt genomic sequence downstream of the *zif-1* stop codon, which was cloned downstream of *pie-1* promoter-driven GFP::H2B in the germline expression vector pID3.01B (Guven-Ozkan et al., 2010; Reese et al., 2000). All deletion constructs were derived from the 771 nucleotide sequence (Guven-Ozkan et al., 2010). The *mex-3* cDNA was cloned downstream of the *med-1* promoter-driven GFP (Maduro et al., 2001).

C. elegans transformation

All integrated lines were generated by microparticle bombardment (Praitis et al., 2001) whereas other transgenic lines were generated by complex array injection (Kelly et al., 1997). The GFP::MEX-3 expressing line was generated by micro-injection. For each construct, expression was analyzed and found to be consistent in at least two independent lines.

RNA interference

Feeding RNAi was performed as described (Timmons and Fire, 1998) using HT115 bacteria seeded on NGM plates containing 1 mM IPTG. L1 larvae were fed for 2 days at 25 °C.

Immunofluorescence

Immunofluorescence for *C. elegans* embryos was carried out as described previously: for anti-SPN-4 (1/10,000, rabbit) (Ogura et al., 2003). Secondary antibodies used were Alexa568 conjugated goat anti-rabbit (Invitrogen, 1/250).

RNA binding assay

MBP-tagged proteins were prepared by cloning individual cDNAs into pDEST-MAL (Invitrogen). These expression clones were transformed into Rosetta cells, induced with 1 mM IPTG for 4 h at room temperature in the presence of 0.2% glucose and 0.1 mM zinc, purified by amylose resin (NEB) as previously described (Nishi and Lin, 2005), and eluted with 50 mM maltose.

Biotinylation of RNA and pull-downs were performed as previously described (Guven-Ozkan et al., 2010; Lee and Schedl, 2001) except for the following modifications. The optimal amount of purified protein and the *zif-1* 3′ UTR were empirically determined by titration series. Each binding reaction contained 150 ng of the purified MBP-tagged protein and 100 ng/60 nucleotides of biotinylated RNA. For the competition binding assay shown in Fig. 2D, 1 μg of each MBP-tagged protein and 30 ng/60 nt RNA were used.

Analysis of embryos, imaging, and quantification

All images except those shown in Fig. 6A were obtained with an Axioplan microscope (Zeiss) equipped with a MicroMax-512EBFT CCD camera (Princeton Instruments) controlled by the Metamorph acquisition software (Molecular Devices) (Guven-Ozkan et al., 2008). Imaging for Fig. 6A was performed with a LSM 510 Meta confocal microscope (Zeiss) and quantified with ImageJ software (Guven-Ozkan et al., 2008). Nuclear GFP intensity was quantified for cells in 28-cell embryos. Embryos were imaged at multiple time points to evaluate the expression of GFP::MEX-3 at 12–16-cell stages and the levels of GFP at 20–50-cell stages. The ratios of nuclear GFP intensities in EMS descendants to that in AB descendants for individual embryos were plotted in Fig. 6B.

Supplementary materials related to this article can be found online at doi:10.1016/j.ydbio.2012.01.002.

Acknowledgments

The authors would like to thank Lin lab members for discussions, Lesilee Rose for *spn-2* cDNA, Kuppuswamy Subramaniam and Geraldine Seydoux for the germline expression vector, Geraldine Seydoux for JH1436, Yuji Kohara for the anti-SPN-4 antibody, Wormbase for valuable information, and *C. elegans* Genetics Center (CGC) for various strains. This work was supported by NIH grants (HD37933 and GM84198) to R. L.

References

Batchelder, C., Dunn, M.A., Choy, B., Suh, Y., Cassie, C., Shim, E.Y., Shin, T.H., Mello, C., Seydoux, G., Blackwell, T.K., 1999. Transcriptional repression by the *Caenorhabditis elegans* germ-line protein PIE-1. Genes Dev. 13, 202–212.

Cheng, K.C., Klancer, R., Singson, A., Seydoux, G., 2009. Regulation of MBK-2/DYRK by CDK-1 and the pseudophosphatases EGG-4 and EGG-5 during the oocyte-to-embryo transition. Cell 139, 560–572.

DeRenzo, C., Reese, K.J., Seydoux, G., 2003. Exclusion of germ plasm proteins from somatic lineages by cullin-dependent degradation. Nature 424, 685–689.

Detwiler, M.R., Reuben, M., Li, X., Rogers, E., Lin, R., 2001. Two zinc finger proteins, OMA-1 and OMA-2, are redundantly required for oocyte maturation in *C. elegans*. Dev. Cell 1, 187–199.

Draper, B.W., Mello, C.C., Bowerman, B., Hardin, J., Priess, J.R., 1996. MEX-3 is a KH domain protein that regulates blastomere identity in early *C. elegans* embryos. Cell 87, 205–216.

Farley, B.M., Pagano, J.M., Ryder, S.P., 2008. RNA target specificity of the embryonic cell fate determinant POS-1. RNA 14, 2685–2697.

Ghosh, D., Seydoux, G., 2008. Inhibition of transcription by the *Caenorhabditis elegans* germline protein PIE-1: genetic evidence for distinct mechanisms targeting initiation and elongation. Genetics 178, 235–243.

Guedes, S., Priess, J.R., 1997. The *C. elegans* MEX-1 protein is present in germline blastomeres and is a P granule component. Development 124, 731–739.

Guven-Ozkan, T., Nishi, Y., Robertson, S.M., Lin, R., 2008. Global transcriptional repression in *C. elegans* germline precursors by regulated sequestration of TAF-4. Cell 135, 149–160.

Guven-Ozkan, T., Robertson, S.M., Nishi, Y., Lin, R., 2010. zif-1 translational repression defines a second, mutually exclusive OMA function in germline transcriptional repression. Development 137, 3373–3382.

Huang, N.N., Mootz, D.E., Walhout, A.J., Vidal, M., Hunter, C.P., 2002. MEX-3 interacting proteins link cell polarity to asymmetric gene expression in *Caenorhabditis elegans*. Development 129, 747–759.

Kelly, W.G., Xu, S., Montgomery, M.K., Fire, A., 1997. Distinct requirements for somatic and germline expression of a generally expressed *Caenorhabditis elegans* gene. Genetics 146, 227–238.

Lee, M.H., Schedl, T., 2001. Identification of in vivo mRNA targets of GLD-1, a maxi-KH motif containing protein required for *C. elegans* germ cell development. Genes Dev. 15, 2408–2420.

Li, W., DeBella, L.R., Guven-Ozkan, T., Lin, R., Rose, L.S., 2009. An eIF4E-binding protein regulates katanin protein levels in C. elegans embryos. J Cell Biol 187, 33–42.

Lin, R., 2003. A gain-of-function mutation in oma-1, a *C. elegans* gene required for oocyte maturation, results in delayed degradation of maternal proteins and embryonic lethality. Dev. Biol. 258, 226–239.

Maduro, M.F., Meneghini, M.D., Bowerman, B., Broitman-Maduro, G., Rothman, J.H., 2001. Restriction of mesendoderm to a single blastomere by the combined action of SKN-1 and a GSK-3beta homolog is mediated by MED-1 and -2 in *C. elegans*. Mol. Cell 7, 475–485.

Mello, C.C., Draper, B.W., Krause, M., Weintraub, H., Priess, J.R., 1992. The pie-1 and mex-1 genes and maternal control of blastomere identity in early *C. elegans* embryos. Cell 70, 163–176.

Mello, C.C., Schubert, C., Draper, B., Zhang, W., Lobel, R., Priess, J.R., 1996. The PIE-1 protein and germline specification in *C. elegans* embryos. Nature 382, 710–712.

Merritt, C., Rasoloson, D., Ko, D., Seydoux, G., 2008. 3′ UTRs are the primary regulators of gene expression in the *C. elegans* germline. Curr. Biol. 18, 1476–1482.

Nakamura, A., Seydoux, G., 2008. Less is more: specification of the germline by transcriptional repression. Development 135, 3817–3827.

Nishi, Y., Lin, R., 2005. DYRK2 and GSK-3 phosphorylate and promote the timely degradation of OMA-1, a key regulator of the oocyte-to-embryo transition in *C. elegans*. Dev. Biol. 288, 139–149.

Ogura, K., Kishimoto, N., Mitani, S., Gengyo-Ando, K., Kohara, Y., 2003. Translational control of maternal glp-1 mRNA by POS-1 and its interacting protein SPN-4 in *Caenorhabditis elegans*. Development 130, 2495–2503.

Pagano, J.M., Farley, B.M., McCoig, L.M., Ryder, S.P., 2007. Molecular basis of RNA recognition by the embryonic polarity determinant MEX-5. J. Biol. Chem. 282, 8883–8894.

Pagano, J.M., Farley, B.M., Essien, K.I., Ryder, S.P., 2009. RNA recognition by the embryonic cell fate determinant and germline totipotency factor MEX-3. Proc. Natl. Acad. Sci. U. S. A. 106, 20252–20257.

Praitis, V., Casey, E., Collar, D., Austin, J., 2001. Creation of low-copy integrated transgenic lines in *Caenorhabditis elegans*. Genetics 157, 1217–1226.

Reese, K.J., Dunn, M.A., Waddle, J.A., Seydoux, G., 2000. Asymmetric segregation of PIE-1 in *C. elegans* is mediated by two complementary mechanisms that act through separate PIE-1 protein domains. Mol. Cell 6, 445–455.

Schaner, C.E., Deshpande, G., Schedl, P.D., Kelly, W.G., 2003. A conserved chromatin architecture marks and maintains the restricted germ cell lineage in worms and flies. Dev. Cell 5, 747–757.

Schubert, C.M., Lin, R., de Vries, C.J., Plasterk, R.H., Priess, J.R., 2000. MEX-5 and MEX-6 function to establish soma/germline asymmetry in early *C. elegans* embryos. Mol. Cell 5, 671–682.

Seydoux, G., Dunn, M.A., 1997. Transcriptionally repressed germ cells lack a subpopulation of phosphorylated RNA polymerase II in early embryos of *Caenorhabditis elegans* and *Drosophila melanogaster*. Development 124, 2191–2201.

Seydoux, G., Fire, A., 1994. Soma-germline asymmetry in the distributions of embryonic RNAs in *Caenorhabditis elegans*. Development 120, 2823–2834.

Shirayama, M., Soto, M.C., Ishidate, T., Kim, S., Nakamura, K., Bei, Y., van den Heuvel, S., Mello, C.C., 2006. The conserved kinases CDK-1, GSK-3, KIN-19, and MBK-2 promote OMA-1 destruction to regulate the oocyte-to-embryo transition in *C. elegans*. Curr. Biol. 16, 47–55.

Stitzel, M.L., Pellettieri, J., Seydoux, G., 2006. The *C. elegans* DYRK kinase MBK-2 marks oocyte proteins for degradation in response to meiotic maturation. Curr. Biol. 16, 56–62.

Strome, S., Specification of the germ line (July 28, 2005), WormBook, ed. The C. elegans Research Community, WormBook, doi/10.1895/-wormbook.1.9.1, http://www.wormbook.org.

Strome, S., Lehmann, R., 2007. Germ versus soma decisions: lessons from flies and 779 worms. Science 316, 392–393.

Tabara, H., Hill, R.J., Mello, C.C., Priess, J.R., Kohara, Y., 1999. pos-1 encodes a cytoplasmic zinc-finger protein essential for germline specification in *C. elegans*. Development 126, 1–11.

Tenenhaus, C., Schubert, C., Seydoux, G., 1998. Genetic requirements for PIE-1 localization and inhibition of gene expression in the embryonic germ lineage of *Caenorhabditis elegans*. Dev. Biol. 200, 212–224.

Tenlen, J.R., Schisa, J.A., Diede, S.J., Page, B.D., 2006. Reduced dosage of pos-1 suppresses Mex mutants and reveals complex interactions among CCCH zinc-finger proteins during *Caenorhabditis elegans* embryogenesis. Genetics 174, 1933–1945.

Timmons, L., Fire, A., 1998. Specific interference by ingested dsRNA. Nature 395, 854.

Zhang, F., Barboric, M., Blackwell, T.K., Peterlin, B.M., 2003. A model of repression: CTD analogs and PIE-1 inhibit transcriptional elongation by P-TEFb. Genes Dev. 17, 748–758.